Thin Solid Films 519 (2011) 7712–7716

Contents lists available at ScienceDirect

Thin Solid Films

journal homepage: www.elsevier.com/locate/tsf

Preparation of nanoporous polyimide thin films via layer-by-layer self-assembly of cowpea mosaic virus and poly(amic acid)

Bo Peng [a], Guojun Wu [a], Yuan Lin [a], Qian Wang [b], Zhaohui Su [a,*]

[a] State Key Laboratory of Polymer Physics and Chemistry, Changchun Institute of Applied Chemistry, Chinese Academy of Sciences, Changchun, Jilin 130022, PR China
[b] Department of Chemistry and Biochemistry, University of South Carolina, Columbia, SC, 29208, USA

ARTICLE INFO

Article history:
Received 5 July 2010
Received in revised form 18 May 2011
Accepted 18 May 2011
Available online 25 May 2011

Keywords:
Multilayers
Self-assembly
Dielectric constants
Cowpea mosaic virus
Polyimides

ABSTRACT

Low dielectric (low-κ) materials are of key importance for the performance of microchips. In this study, we show that nanosized cowpea mosaic virus (CPMV) particles can be assembled with poly(amic acid) (PAA) in aqueous solutions via the layer-by-layer technique. Then, upon thermal treatment CPMV particles are removed and PAA is converted into polyimide in one step, resulting in a porous low-κ polyimide film. The multilayer self-assembly process was monitored by quartz crystal microbalance and UV–Vis spectroscopy. Imidization and the removal of the CPMV template was confirmed by Fourier transform infrared spectroscopy and atomic force microscopy respectively. The dielectric constant of the nanoporous polyimide film thus prepared was 2.32 compared to 3.40 for the corresponding neat polyimide. This work affords a facile approach to fabrication of low-κ polyimide ultrathin films with tunable thickness and dielectric constant.

1. Introduction

In recent years, many studies have focused on fabrication of materials with low dielectric constants (low-κ), which are important for the microelectronics industry because they enhance signal speed and improve the performance of microchips [1,2]. Due to its excellent mechanical properties and thermal stability, polyimide has become a promising candidate for low-κ materials for the application as intermetal dielectrics [1]. Typical polyimides have a relative dielectric constant of ~3.4, which can be reduced by introducing air gaps (pores) [3–5]. Pores can be introduced via high-temperature foaming, but the structure generated by this method is not homogeneous and is covered with dense surface layers. Nanoporous polyimide films can also be produced from phase-separated blends with poly(propylene oxide) (PPO). The thermally mobile PPO can form homogenous spherical domains in the polyimide matrix, which are then eliminated by heating the blend films to above 300 °C, leaving nanosized pores in the polyimide thin films [4,5]. It has been reported that silica or Al_2O_3 can be incorporated into polyimide films by the sol-gel route, and by etching the silica particles with HF porous films are obtained, which exhibit significantly decreased dielectric constants compared to pure polyimide films [6–8]. Another interesting approach to decrease dielectric constants is to introduce polyhedral oligomeric silsequioxane (POSS) nanoporous moieties as chain-ends, grafted side chains, and pendant groups onto the polyimide molecules [9–11]. Nevertheless, it is still a challenge to fabricate porous polyimide thin films less than 50 nm thick via convenient solution-based processes such as spinning or casting.

Layer-by-layer deposition is a versatile method for fabricating ultra-thin films, where polyelectrolytes of opposite charges are alternatingly deposited onto a substrate, and the structure, thickness, and composition of the thin films can be conveniently adjusted by controlling the assembling conditions. In addition to polyelectrolytes, many other charged species such as clay, silica, virus, protein, and POSS particles have been assembled by this layer-by-layer assembly process [12–18]. Cowpea mosaic virus (CPMV) is a plant virus with a diameter of ~30 nm. Its physical, biological and genetic properties have been well characterized over the past few years. The virus comprises 60 copies of two protein subunits in an icosahedral symmetry. The particles are monodisperse, remarkably stable, and have been used as a model system in bioconjugation chemistry [19]. It has been demonstrated that CPMV particles can be efficiently incorporated into thin films through the layer-by-layer assembly technique [20,21]. In this paper, we use CPMV particles as a nanosized pore generating motif and take advantage of the solubility and anionic characteristic of poly(amic acid) (PAA), the precursor polymer of polyimide, to assemble multilayer thin films from CPMV with PAA. Then upon thermal treatment, the CPMV particles are removed and the PAA is converted into polyimide in one step, resulting in porous low-κ polyimide thin films.

* Corresponding author. Tel.: +86 431 85262854; fax: +86 431 85262126.
E-mail address: zhsu@ciac.jl.cn (Z. Su).

0040-6090/$ – see front matter © 2011 Elsevier B.V. All rights reserved.
doi:10.1016/j.tsf.2011.05.047

2. Experimental procedure

2.1. Materials

Dimethylacetamide (DMAc, Beijing Chemical Reagents Company) was distilled from phosphorus pentoxide. 4,4′-oxydianiline (ODA) and pyromellitic dianhydride (PMDA) were synthesized in our laboratory and purified by sublimation under reduced pressure prior to use. Poly(diallyldimethylammonium chloride) (PDDA, 20 wt.% in water, $M_w = 200{,}000–350{,}000$), and poly(allylamine hydrochloride) (PAH, $M_w = 70{,}000$) were purchased from Sigma-Aldrich and used as received. Cowpea mosaic virus (CPMV) was harvested and purified as described previously [20]. Deionized water (18.2 MΩ·cm) was obtained from a Millipore Simplicity 185 purification unit and used for rinsing and preparation of all solutions. Solution pH was adjusted by 0.1 M HCl and NaOH aqueous solutions.

2.2. Preparation of poly(amic acid) (PAA)

PAA was prepared following a literature procedure [22]. In a typical experiment, 20 mL dimethylacetamide (DMAc) were added 0.918 g 4,4′-oxydianiline (ODA) and 1.000 g pyromellitic dianhydride (PMDA) while stirring at room temperature. After 24 h, a clear light yellow PAA solution was obtained with a concentration of ~10%. Three milliliters of the PAA solution were slowly added to ~300 mL acetone to yield a flocculent deposit, which was filtered, washed with acetone, and dried under vacuum for about 20 h. The PAA was dissolved in water by adding triethylamine to the mixture. The solution became clear at pH greater than 7.0.

2.3. Substrate preparation

Quartz slides were cleaned in a piranha solution (H_2SO_4 (98%)-H_2O_2 (30%) 70:30, v/v) for 40 min, and rinsed with deionized water. The slides were then immersed in a mixture of $NH_3 \cdot H_2O$ (25%)-H_2O_2 (30%) (50:50, v/v) for 30 min, removed and rinsed again with deionized water, and dried with nitrogen. The quartz slides were used as the substrate for UV study of assembled thin films. Glass slides were cleaned using the above procedure, and then sputtered with 15 nm Cr and 100 nm Au, and used as the substrates for reflection–absorption Fourier transform infrared spectroscopy (FTIR) study of the assembled thin films. Ag-coated quartz electrodes were cleaned with ethanol and water for 1 min respectively, and dried with nitrogen, and used as the sensor for quartz crystal microgravimetry (QCM) measurements.

2.4. Assembly of the multilayer composite films

A quartz or glass slide was immersed in a PDDA (or PAH) solution (1.0 mg/mL) for about 1 h, removed and rinsed with deionized water, and then immersed in a PAA solution (1.0 mg/mL, pH = 9.0) for 12 min, removed and rinsed with deionized water. The cycle was repeated until a desired number of layers was obtained. Then the substrate was immersed in a CPMV solution (pH = 7.0 in potassium phosphate buffer) for about 15 min, removed and rinsed with water. Next additional PDDA/PAA or PAH/PAA layers were assembled on top of the CPMV layer until a desired number of layers was reached. Finally, the film was dried with a stream of nitrogen.

2.5. Thermal treatment of the multilayer films

A multilayer film composed of $(PAH/PAA)_5[PAH/CPMV/(PAH/PAA)_4]_3$ and assembled on a gold-coated silicon slide was heated at 275 °C for 2 h in air to both affect cross-linking [23] and remove the CPMV particles.

2.6. Characterization

The PAA was dissolved in DMAc and the solution was cast on a KBr disk. The residual solvent was removed under vacuum, and IR spectra of the PAA were obtained on a Bruker Vertex 70 FTIR spectrometer equipped with a deuterated-triglycine-sulfate detector. The spectra were collected at 4 cm^{-1} resolution and 64 scans, and were baseline-corrected using the OPUS software. Reflection–absorption FTIR spectra were collected on a Bruker IFS 66v spectrometer equipped with a MCT detector and a grazing angle reflection accessory (PIKE Technologies) with the incidence angle set at 80°. The resolution was maintained at 4 cm^{-1} and 256 scans were co-added for each spectrum. UV–Vis spectra were collected on a Shimadzu UV-2450 spectrophotometer. A home-made quartz crystal microbalance (QCM) was used to detect the mass of the deposited layer using a 9 MHz quartz electrode coated with Ag on both sides. QCM frequency shifts were monitored with a Protek C3100 universal frequency counter, and mass of the deposited layer was calculated from the Sauerbrey equation [24],

$$\Delta m = -\frac{\rho_q l_q}{f_0}\frac{\Delta f}{n}$$

where f_0 is the fundamental frequency, ρ_q and l_q are the density and thickness of the quartz crystal, and n is the overtone number. The Sauerbrey equation can be written as $\Delta m = -C\,\Delta f$, where C is mass sensitivity, which was 2.7 ng/cm^2 in our experiments. Ellipsometric measurements were performed by null ellipsometry using a Spectroscopic Ellipsometer (HORIBA Jobin Yvon) with a scanning range of 300–800 nm and a 70° incidence angle. The refractive index of the silicon wafer was 3.882 + 0.019i [3], and that of the silica top layer was 1.457 with the imaginary part set at zero. For each sample three points were measured and then averaged. Atomic force microscopy (AFM) was performed on a Seiko SPA300HV/SPI3800N microscope operating in tapping mode at room temperature.

3. Results and discussion

Fig. 1 displays the FTIR spectrum of the PAA synthesized from ODA and PMDA. The peak at 1659 cm^{-1} represents the C═O stretching vibration of amide I, and the peak at 1545 cm^{-1} is the amide II band from the N–H bending and C–N stretching vibrations. The bands at 1607 and 1406 cm^{-1} are characteristic of the carboxyl. In the high frequency region, the broad band at 3266 cm^{-1} is due to the N–H stretching vibration. These spectral features are consistent with that reported in literature [25], which confirms the structure of the molecule synthesized. Because different substrates were used in this work, such as quartz slides, Ag coated quartz electrodes, Si wafers, and

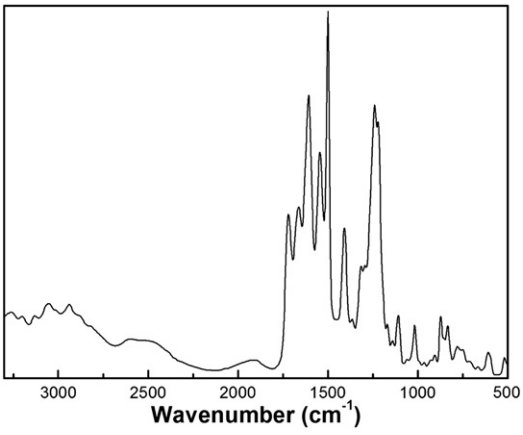

Fig. 1. FTIR spectrum of the PAA synthesized from ODA and PMDA.

gold coated Si wafers, three PDDA/PAA or PAH/PAA bilayers were first assembled on the substrates to create a consistent surface environment for subsequent deposition. PAA synthesized from ODA and PMDA can be dissolved in water under basic condition, where it becomes a polyanion and can be assembled via the layer-by-layer technique. Triethylamine was chosen as the base for this purpose because it can be readily removed from the assembled film at elevated temperature. Since the isoelectric point of CPMV is around 5.2 [19], it carries negative charges at pH 7 or higher. In order to assemble PAA with CPMV, a polycation such as PDDA or PAH was used as the interlayer material. The diameter of CPMV particles is ~30 nm, which is much greater than the thickness of a typical assembled polyelectrolyte layer. In order to maintain the void fraction at a reasonable level, multiple PAA/PDDA or PAA/PAH bilayers were deposited in between two CPMV layers. The mass increase during the deposition process is shown in Fig. 2 as indicated by the QCM frequency shifts. The average frequency change for a PDDA and a PAA layer is 27 and 32 Hz, respectively. By applying the Sauerbrey equation discussed in Section 2.6, these frequency shifts correspond to a mass increase of 72.0 and 86.4 ng/cm^2 for a PDDA and PAA layer, respectively. Assuming a density of 1 g/cm^3, the thickness of one PDDA/PAA bilayer is estimated to be 1.6 nm. In addition, the average frequency shift associated with each CPMV assembly is 147 ± 1 Hz, suggesting that the deposition of CPMV under this condition (0.05 mg/mL in pH = 7 buffer) is very reproducible. The frequency shift corresponds to ~396 ng/cm^2 of CPMV deposited on each side of the QCM electrode as calculated by the Sauerbrey equation. This mass increase in turn corresponds to a 43% coverage of the electrode surface assuming monolayer adsorption with spherical packing. The assembly process was also monitored by UV–Vis. Fig. 3a shows the spectra of multilayer films assembled on quartz slides with compositions of $(PDDA/PAA)_3/[PDDA/CPMV/(PDDA/PAA)_4]_n$ (n = 0–2), where $(PDDA/PAAs)_3$ indicates the precursor films. Because PDDA in solution has only slight absorbance in the UV region [26], the UV absorption of the composite films in the 190–400 nm region is primarily attributed to CPMV and PAA, in particular the π-π^* transition of phenyl rings in PAA at 195 nm and 260 nm. The inset displays the UV absorptions at these two wavelengths against the number of assembly cycle, and a linear growth pattern is observed. This indicates that the adsorption of CPMV and PDDA/PAA was steady and uniform. A similar trend was found for the CPMV/PAA assembly using PAH as the interlayers, as shown in Fig. 3b. For $(PAH/PAAs)_3/[PAH/CPMV/(PAH/PAA)_3]_n$ (n = 0–3) multilayers, the UV absorbance increases linearly with the assembly cycle (Fig. 3b inset), which is consistent with that observed by QCM (data not shown). This indicates that both PAH and PDDA as interlayer polyeletrolytes behave similarly in the assembly process, following a linear growth pattern. In a PDDA/PAA multilayer the

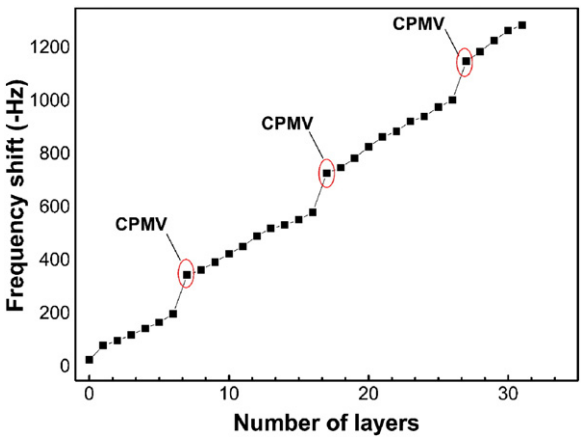

Fig. 2. QCM frequency shifts for the deposition of CPMV, PDDA and PAA. The circles are CPMV, the odd layers are PAA, and the even layers are PDDA.

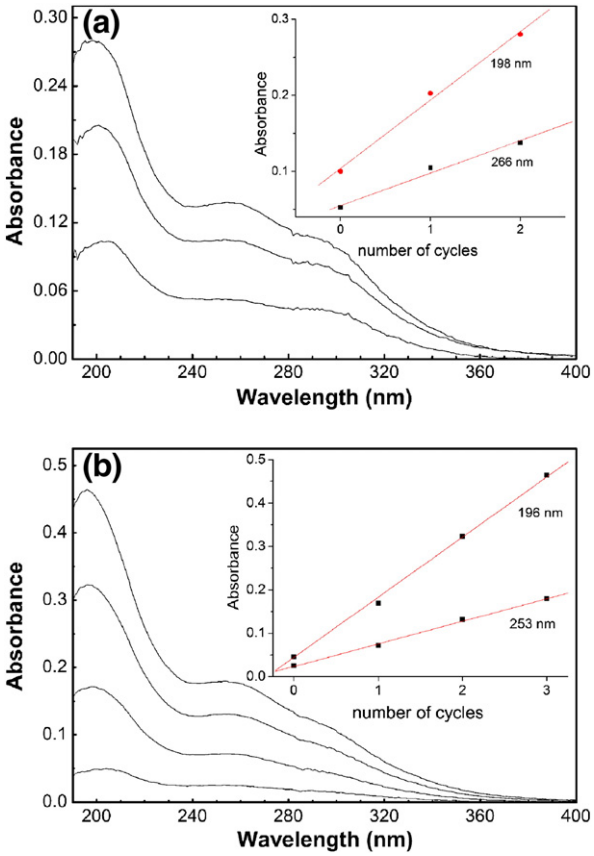

Fig. 3. UV–Vis spectra of the composite multilayer films with different assembly cycles: (a) $(PDDA/PAA)_3/[PDDA/CPMV/(PDDA/PAA)_4]_n$ (n = 0–2), and (b) $(PAH/PAA)_3/[PAH/CPMV/(PAH/PAA)_3]_n$ (n = 0–3). The insets are the absorption peak intensities vs the assembly cycle.

ammonium group in PDDA only forms ionic bond with the carboxyl in PAA, whereas in a PAH/PAA multilayer the amine in PAH can further react with the PAA carboxyl upon heating to form an amide, and the cross linking via the covalent bonds between PAH and PAA layers can significantly improve the stability of the multilayer film [23]. Therefore PAH/PAA pair was chosen as the interlayer for the subsequent fabrication of nanoporous polyimide films.

For these composite films, it is obvious that the dielectric constant is dependent on the amount of the CPMV particles, i.e. the voids, incorporated. Fig. 4 displays the frequency shift detected by QCM associated with one CPMV layer deposited as a function of the CPMV concentration in the solution. It can be seen that the QCM frequency shift, which is proportional to the mass of CPMV deposited on the surface, increases with CPMV solution concentration. This result indicates that the amount of CPMV particles in the composite can be tuned by controlling its solution concentration. On the other hand, CPMV content in the composite can be tuned by changing the number of PDDA/PAA (or PAH/PAA) layers assembled between two CPMV layers. Apparently, as the number of assembled PDDA/PAA (or PAH/PAA) layers in the film increases, CPMV content in the resulting composite film decreases. Therefore, these provide convenient handles for manipulating the dielectric constant of the polyimide films.

It is well known that PAA can be converted into polyimide at elevated temperatures. Fig. 5 shows reflection absorption FTIR spectra of a PAA/CPMV composite film deposited on a gold-coated silicon wafer before and after being heated at 275 °C for 2 h in air. Broad and overlapping bands are observed in the spectrum before the thermal treatment in the region of 1680–1520 cm^{-1}, which are due to the amide bands and asymmetric stretching of $-COO^-$ in the PAA. CPMV, which is comprised of protein, also has amide bands in this region.

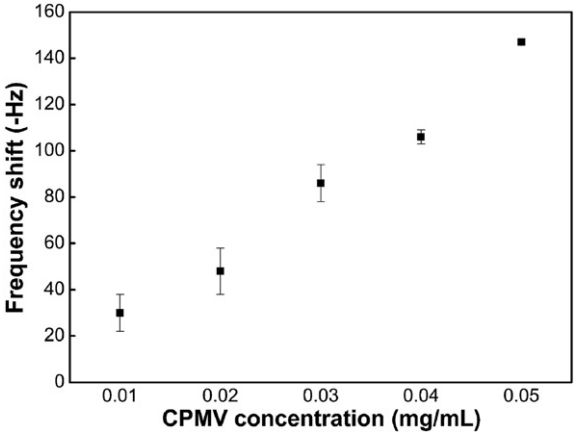

Fig. 4. Dependence of QCM frequency shift associated with the deposition of one CPMV layer on CPMV solution concentration.

After the heat treatment these bands almost completely disappear, and two new bands are observed at 1778 and 1728 cm^{-1}, which are consistent with asymmetric and symmetric carbonyl stretchings of imides [27,28]. This is a clear indication that PAA has been converted into polyimide via thermal imidization.

In order to assess effects of the thermal treatment on the CPMV particles, one CPMV layer was assembled on the surface of a $(PAH/PAA)_5$ multilayer, and heated under the same condition. Fig. 6a is the AFM height image of the surface of the film as assembled. Granular CPMV nanoparticles are clearly identified in the image, and their sizes are ~50 nm, greater than that of the spherical CPMV, which is 30 nm. This indicates that the particles were flattened and collapsed to some extent after drying. These features are absent after the thermal treatment of the same film (Fig. 6b). This result indicates that the CPMV nanoparticles incorporated in the composite films can be completely removed after heating in air at 275 °C for 2 h.

Table 1 lists thicknesses and refractive indexes measured by ellipsometry of three replicate PAA/CPMV composite films, each containing three CPMV layers. As mentioned above, the diameter of a CPMV particle is ~30 nm. However, the average thickness of a composite film with 3 CPMV layers incorporated was only 68.6 nm, instead of the expected 79 nm which assumes perfect spherical packing of the 3 CPMV layers. This suggests that the CPMV particles assembled in the composite multilayers are flattened or collapsed to some extent. This is consistent with the AFM data shown in Fig. 6a. After imidization and removal of the CPMV particles at 275 °C for an extended period of time, average film thickness decreased by ~3 nm to 65.9 nm. This slight shrinkage in the total volume of the film implies that the flattened CPMV particles are largely converted into voids without significant collapse of the porous formed structure after

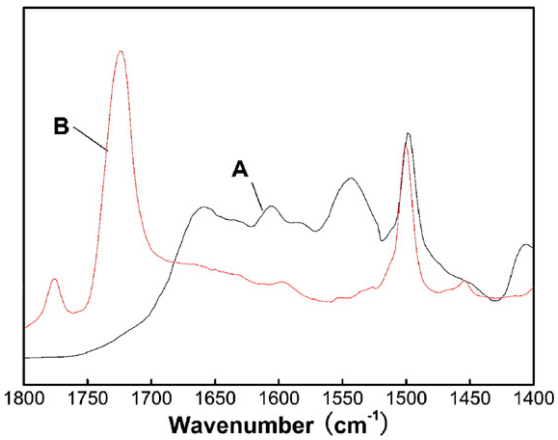

Fig. 5. Reflection–absorption FTIR spectra of a CPMV/PAA composite multilayer with PAH as the interlayers (A) before and (B) after being heated at 275 °C in air for 2 h.

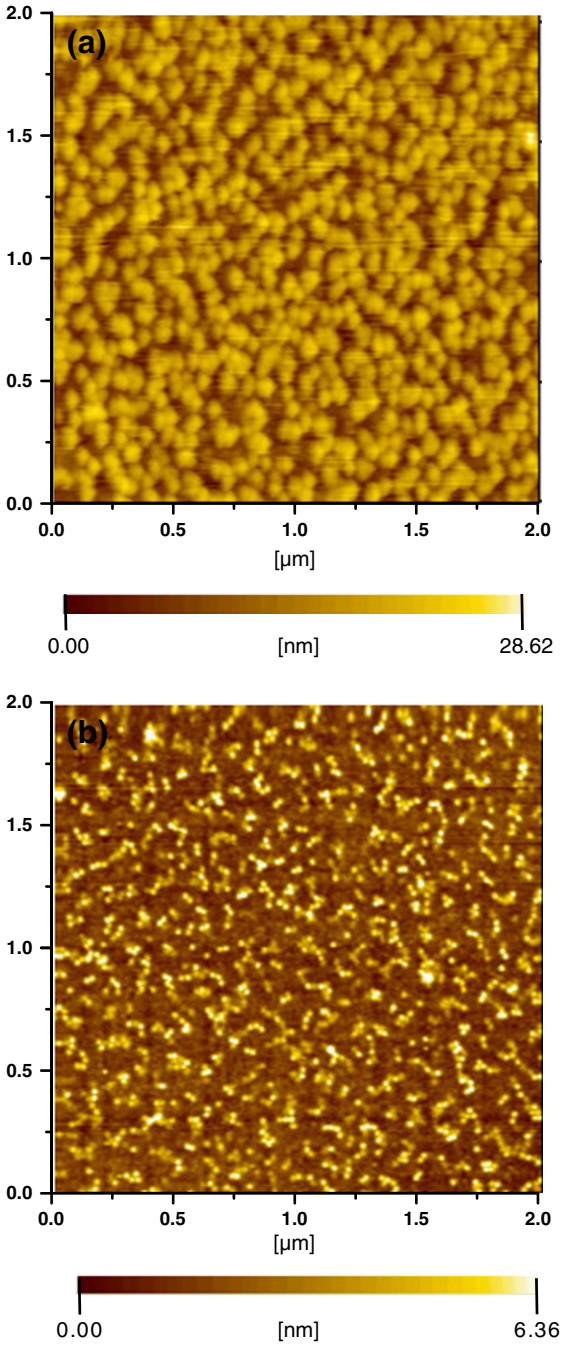

Fig. 6. AFM height images of a $(PAH/PAA)_5$/CPMV multilayer film (a) before and (b) after being heated at 275 °C in air for 2 h.

Table 1
Thicknesses and refractive indexes of $(PAH/PAA)_5/[PAH/CPMV/(PAH/PAA)_{10}]_3$ multilayer films before and after being heated at 275 °C in air for 2 h.

		1	2	3	Average
Before heating	d (nm)	68.5 ± 2.1	68.7 ± 2.0	68.7 ± 2.0	68.6 ± 2.0
	n	1.468	1.467	1.471	1.469 ± 0.002
After heating	d (nm)	65.9 ± 2.1	65.4 ± 2.1	66.2 ± 2.2	65.9 ± 2.2
	n	1.425	1.422	1.414	1.420 ± 0.005

the thermal treatment. The voids incorporated in the film also led to a decrease of the dielectric constant of the film, as indicated by reduction in the refractive index determined by ellipsometry. As shown in Table 1, the refractive index is 1.469 for the composite multilayer containing CPMV nanoparticles, which is further reduced to 1.420 after the CPMV particles were removed. The dielectric constant of a film can be obtained on the basis of refractive index by applying the Maxwell equation, $\varepsilon \approx \eta^2$, with the frequency dispersions correction, $\Delta\varepsilon \approx 0.3$ [29]. The dielectric constant thus derived for the nanoporous polyimide film was 2.32, which is significantly lower than 3.40 for the neat polyimide films [9]. This great decrease is due to incorporation of nanopores generated using CPMV particles as a template.

4. Conclusion

In summary, nanoporous polyimide films can be readily prepared by incorporating virus nanoparticles into composite films via layer-by-layer self-assembly of cowpea mosaic virus (CPMV) with poly (amic acid) (PAA) in aqueous, followed by imidization and removal of the CPMV particles simultaneously upon thermal treatment. The nanopores generated by CPMV particles in the polyimide thin film resulted in a lower dielectric constant of 2.32 compared to 3.40 of neat polyimide. It is possible to tune the dielectric constant of a polyimide film by controlling quantity of virus nanoparticles incorporated into the thin film. This method provides a facile approach to fabrication of ultrathin polyimide films with low dielectric constants.

Acknowledgement

This work was supported by the National Natural Science Foundation of China (20423003). Z.S. thanks the NSFC Fund for Creative Research Groups (50921062) for support.

References

[1] G. Maier, Prog. Polym. Sci. 26 (2001) 3.
[2] H. Treichel, G. Ruhl, P. Ansmann, R. Wurl, C. Muller, M. Dietlmeier, Microelectron. Eng. 40 (1998) 1.
[3] M.R. Baklanov, K. Maex, Phil. Trans. R. Soc. A 364 (2006) 201.
[4] J.L. Hedrick, T.P. Russell, J. Labadie, M. Lucas, S. Swanson, Polymer 36 (1995) 2685.
[5] K.R. Carter, R.A. DiPietro, M.I. Sanchez, S.A. Swanson, Chem. Mater. 13 (2001) 213.
[6] L.W. Hrubesh, L.E. Keene, V.R. Latorre, J. Mater. Res. 8 (1993) 1736.
[7] C.C. Cho, D.M. Smith, J. Anderson, Mater. Chem. Phys. 42 (1995) 91.
[8] P. Ma, W. Nie, Z. Yang, P. Zhang, G. Li, Q. Lei, L. Gao, X. Ji, M. Ding, J. Appl. Polym. Sci. 108 (2008) 705.
[9] C.M. Leu, G.M. Reddy, K.H. Wei, C.F. Shu, Chem. Mater. 15 (2003) 2261.
[10] C.M. Leu, Y.T. Chang, K.H. Wei, Chem. Mater. 15 (2003) 3721.
[11] Y.W. Chen, E.T. Kang, Mater. Lett. 58 (2004) 3716.
[12] E.R. Kleinfeld, G.S. Ferguson, Science 265 (1994) 370.
[13] N.F. Steinmetz, G. Calder, G.P. Lomonossoff, D.J. Evans, Langmuir 22 (2006) 10032.
[14] D.L. Feldheim, K.C. Grabar, M.J. Natan, T.E. Mallouk, J. Am. Chem. Soc. 118 (1996) 7640.
[15] K. Ariga, Y. Lvov, T. Kunitake, J. Am. Chem. Soc. 119 (1997) 2224.
[16] J.J. Yuan, S.X. Zhou, B. You, L.M. Wu, Chem. Mater. 17 (2005) 3587.
[17] T. Cassagneau, F. Caruso, J. Am. Chem. Soc. 124 (2002) 8172.
[18] G. Wu, Z. Su, Chin. J. Appl. Chem. 25 (2008) 270.
[19] A.S. Blum, C.M. Soto, C.D. Wilson, J.D. Cole, M. Kim, B. Gnade, A. Chatterji, W.F. Ochoa, T.W. Lin, J.E. Johnson, B.R. Ratna, Nano Lett. 4 (2004) 867.
[20] Y. Lin, Z. Su, Z. Niu, S. Li, G. Kaur, L.A. Lee, Q. Wang, Acta Biomater. 4 (2008) 838.
[21] N. Li, Z.Q. Deng, Y.A. Lin, X.J. Zhang, Y.H. Geng, D.G. Ma, Z.H. Su, J. Appl. Phys. 105 (2009) 013511.
[22] C. Zhang, Z. Yang, M. Ding, Chin. J. Appl. Chem. 18 (2001) 544.
[23] J.J. Harris, P.M. DeRose, M.L. Bruening, J. Am. Chem. Soc. 121 (1999) 1978.
[24] G. Sauerbrey, Z. Phys. 155 (1959) 206.
[25] Y. Jin, G. Zeng, D. Zhu, Y. Huang, Z. Su, Chin. J. Appl. Chem. 28 (2011) 258.
[26] T. Shutava, M. Prouty, D. Kommireddy, Y. Lvov, Macromolecules 38 (2005) 2850.
[27] D.M. Sullivan, M.L. Bruening, J. Am. Chem. Soc. 123 (2001) 11805.
[28] D.M. Sullivan, M.L. Bruening, Chem. Mater. 15 (2003) 281.
[29] D. Boese, H. Lee, D.Y. Yoon, J.D. Swalen, J.F. Rabolt, J. Polym, Sci., Part B: Polym. Phys. 30 (1992) 1321.